www.ptcer.pl/mccm

MATERIAŁY CERAMICZNE /CERAMIC MATERIALS/, 62, 4, (2010), 545-549

TiO_2-based Nanopowders for Gas Sensor

Marta Radecka[1]*, Marcin Jasiński[1], Joanna Klich-Kafel[1], Mieczysław Rękas[1], Barbara Łysoń[2], Adam Czapla[2], Maria Lubecka[2], Mariusz Sokołowski[2], Katarzyna Zakrzewska[2], Andre Heel[3], Thomas J. Graule[3]

[1] AGH University of Science and Technology, Faculty of Materials Science and Ceramics, Kraków, Poland
[2] AGH University of Science and Technology, Faculty of Electrical Engineering, Automatics, Computer Science and Electronics, Kraków, Poland
[3] EMPA, Swiss Federal Laboratories for Materials Testing and Research, Laboratory for High Performance Ceramics, Uberlandstrasse 129, 8600 Dubendorf, Switzerland
*e-mail: radecka@agh.edu.pl

Abstract

Flame spray synthesis (FSS) was used to grow TiO_2-based nanopowders from which TiO_2:Cr nanosensors were obtained. Structural properties of crystalline TiO_2:Cr nanopowders at different Cr loadings (0.1–5.0 at.%) have been investigated. Material studies have been performed using standard methods: X-ray diffraction (XRD) transmission electron microscopy (TEM) and Brunauer-Emmett-Teller adsorption isotherms analysis (BET). High specific surface area (37-126 m^2/g) and small crystallite size (9-27 nm) have been reached. Incorporation of Cr into TiO_2 lattice affects the specific surface area of nanopowders, the crystallite size and the rutile to anatase ratio. Gas sensing characteristics of TiO_2:Cr nanosensors upon interaction with H_2 have been recorded in the self-assembled experimental system. The detection of hydrogen was carried out over the concentration range of 50-3000 ppm at the temperatures extending from 200 to 400ºC. It is demonstrated that nanomaterials based on TiO_2:Cr are attractive for ultimate sensors applications due to a decrease in the operating temperature down to 210-250ºC, accompanied by an increase in the sensor response. Taking into account the possible operating costs, the best candidates for the commercial use are TiO_2:1 at.% Cr and TiO_2:5 at.% Cr nanosensors.
Keywords: Gas sensors, Nanopowders, TiO_2, Hydrogen detection

OPARTE NA TiO_2 NANOPROSZKI DLA CZUJNIKA GAZU

Do otrzymania nanoproszków dla czujników gazu opartych na TiO_2:Cr zastosowano syntezę płomieniową FSS (*flame spray synthesis*). Określono właściwości strukturalne nanoproszków TiO_2:Cr o różnych stężeniach Cr (0.1–5.0 at.%). Badane materiały scharakteryzowano za pomocą standardowych metod, a mianowicie dyfrakcyjnej analizy rentgenowskiej (XRD), mikroskopii transmisyjnej (TEM) oraz analizy izoterm adsorpcji Brunauer-Emmett-Tellera (BET). Otrzymano materiały o wysokiej powierzchni właściwej (37-126 m^2/g) i rozmiarach krystalitów w zakresie 9-27 nm. Wprowadzenie Cr do sieci TiO_2 wpływa na powierzchnię właściwą nanoproszków, rozmiar krystalitu i stosunek rutylu do anatazu. Do pomiaru charakterystyk nanoczujników TiO_2:Cr w wyniku oddziaływania z H_2 zastosowano specjalnie skonstruowany układ pomiarowy. Wyznaczenie kinetyki zmian oporu elektrycznego spowodowanego zmianą ilości wodoru przeprowadzono w zakresie stężeń 50-3000 ppm H_2 w temperaturach od 200 do 400ºC. Pokazano, że obniżeniu temperatury pracy do 210-250ºC towarzyszy wzrost sygnału pomiarowego, co powoduje, że materiały oparte na TiO_2:Cr są atrakcyjne z punktu widzenia zastosowań w czujnikach gazu. Biorąc pod uwagę przewidywane koszty eksploatacyjne, najlepszymi kandydatami do komercyjnego wykorzystania są nanoczujniki TiO_2:1 at.% Cr oraz TiO_2:5 at.% Cr.
Słowa kluczowe: czujniki gazu, nanoproszki, TiO_2, wykrywanie wodoru

1. Introduction

Transition metal oxides, such as TiO_2, are particularly interesting for their remarkable ability to change the electrical resistivity in response to oxidizing and reducing gases. Reversible and large changes in the electrical resistance (ΔR) along with the inherent stability of these ceramics at high temperatures and in harsh environments are widely exploited in the resistive-type gas sensors based on TiO_2 [1-3]. Basic parameters characterizing gas sensor performance such as sensitivity, selectivity and response time of TiO_2-based sensors can be optimized by choosing the appropriate type and level of doping [4-6]. Doping with Cr is known to reduce the response time and lower the initial resistivity (baseline) of the sensor which facilitates the signal detection [7-9].

Recently, many attempts have been undertaken to exploit the influence of Cr on the electrical and gas sensing properties of titanium dioxide [7-10]. It was demonstrated that the addition of Cr can change the electronic conductivity of TiO_2 from *n*- to *p*-type [11-13]. This is beneficial for detection of

oxidizing gases such as oxygen and NO_x where the sign of the resistance change can be reversed due to the use of *p*-type material [8].

The mechanism of gas sensing involves adsorption/desorption processes at the surfaces, interfaces or grain boundaries. Therefore, nanomaterials with a decreased particle size and increased average specific surface area are highly recommended for gas sensing applications [14-15]. Nanosensors largely benefit from the enhanced density of centers active for chemisorption in such a sense that their sensitivity, selectivity and response time can be significantly improved. Nanosensors are expected to perform at the temperature lower than their microcrystalline counterparts, thereby reducing the power consumption and cost of operation.

In our earlier papers [3, 6], we studied the performance of microcrystalline and thin films sensors based on TiO_2:Cr. In this work we focus our attention on nanocrystalline TiO_2:Cr powders obtained by flame spray synthesis (FSS) and their ultimate application to gas sensing. The aim of this work is to study the structural and gas sensing properties of TiO_2:Cr nanosensors produced from nanopowders synthesized in the flame spray [16]. The determination of both the effect of chromium concentration and that of a decreased crystallite size on the sensor dynamic responses to hydrogen have been the main objectives of our investigations. In this work, we have concentrated on hydrogen sensing for the obvious reasons that monitoring of hydrogen leakage is an indispensable issue for hydrogen fuel cells; hydrogen being the "fuel of the future" [2].

2. Experimental

Nanopowders of TiO_2:Cr with up to 5 at.% Cr were obtained by FSS as described in detail in [16]. Titanium tetra-isopropoxide TTIP and the solution of chromium acetyloacetonate CHAA in *m*-xylene were used as precursors of Ti and Cr, respectively. Nanosensors were prepared in a form of circular tablets by pressing the nanopowder at the pressure of 25 MPa and heating up to 400°C. Planar silver electrodes were applied 5 mm apart. It has been verified in the subsequent measurements that the sensor processing did not change its nanocrystalline nature.

For the characterization of TiO_2:Cr nanopowders standard methods have been used: X-ray diffraction (XRD), transmission electron microscopy (TEM) and Brunauer-Emmett-Teller adsorption isotherms (BET). Crystallographic structure, crystallite size and anatase/rutile weight percentage (W_A) were analyzed on the basis of X-ray diffraction measurements performed on X'Pert MPD Philips diffractometer. TEM images were obtained with a Philips CM30 transmission electron microscope. The primary particle size, shape and distribution of particles were of particular interest. Specific surface area (*SSA*) was determined from nitrogen adsorption isotherms (Brunauer-Emmett-Teller, BET) obtained with a Beckman-Coulter SA3100. Powders were annealed under nitrogen atmosphere at 180ºC for 2 h in order to desorb water from their surface.

Dynamic changes in the electrical resistance, *i.e.*, gas sensor characteristics, were recorded in a self-assembled experimental system shown in Fig. 1. The system consists

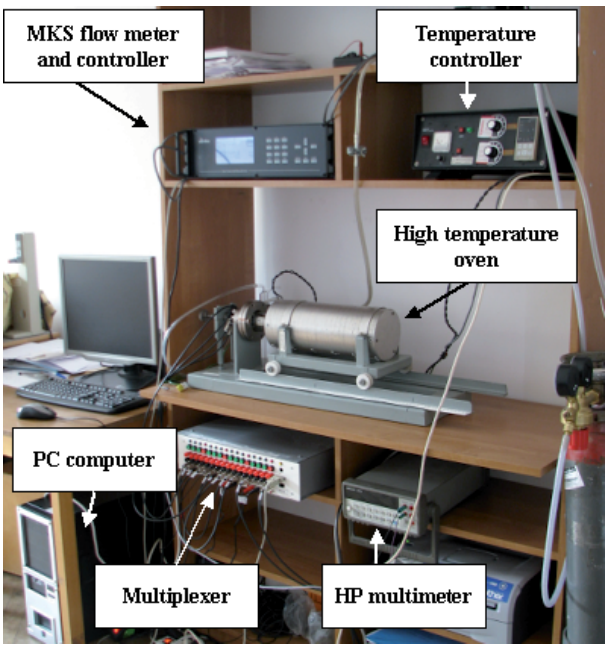

Fig. 1. Experimental set-up for gas sensing measurements.

of the high temperature oven where the sensors are placed, the temperature controller that stabilizes the temperature in the oven, the multiplexer that enables to switch between the measured signals (voltage drop at a Pt-RhPt thermocouple and two sensors resistances at two different current polarizations), gas admission system equipped with MKS flowmeters and a controller, Hewlett Packard HP34401A multimeter for signal recording and PC computer with the implemented LabView program for data acquisition.

Gas sensor response *S* is defined as:

$$S = \frac{R_0 - R}{R_0}, \qquad (1)$$

where R_0 is the electrical resistance (baseline) in the reference gas, *i.e.*, air, while *R* is its current value upon the sensor exposure to the detected gas.

The detection of hydrogen was performed over a low-to-medium concentration range of 50-3000 ppm at temperatures of 200-400ºC.

3. Results and discussion

Table 1. Quantitative results of the structural analysis of TiO_2:Cr nanopowders.

Cr [at.%]	*SSA* [m^2/g]	Crystallite size from XRD [nm]		Anatase content W_A [wt%]
		Anatas	Rutile	
0	37.5	26.8	13.6	94.8
0.10	48.4	21.2	9.6	94.8
0.20	47.6	22.7	11.2	95.2
0.50	72.2	15.7	13.0	92.8
1.00	87.1	13.8	9.3	92.0
5.00	126.6	9.1	7.5	83.8

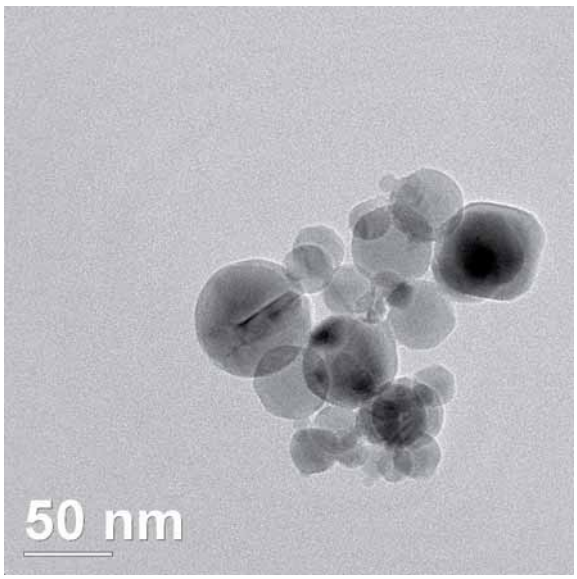

a)

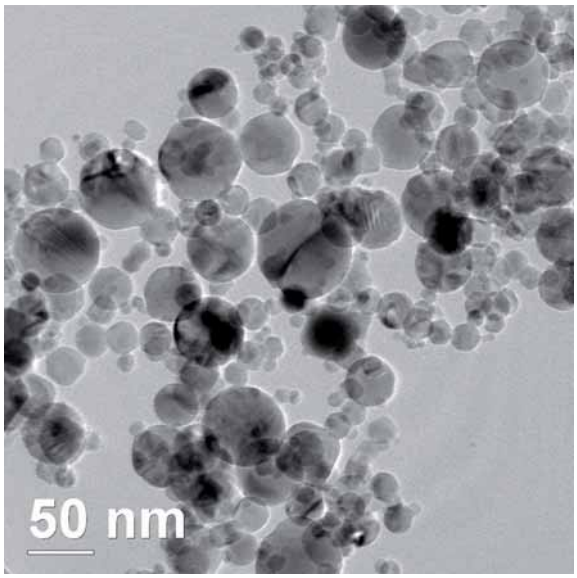

b)

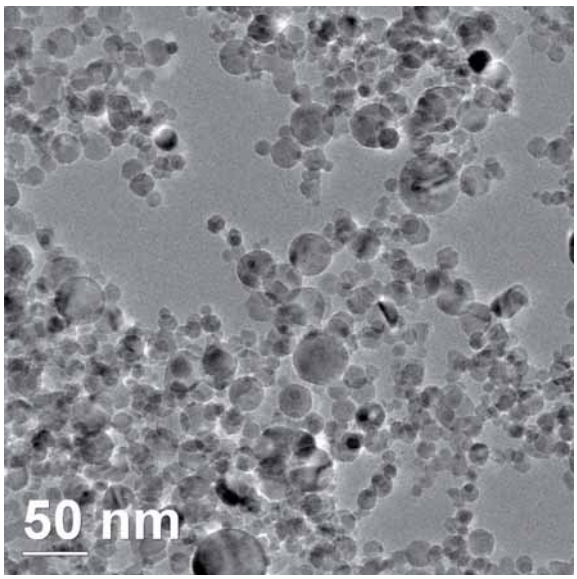

c)

Fig. 2. TEM images of TiO_2:Cr nanopowders at different Cr loadings: a) TiO_2, b) 0.1 at.% Cr, c) 1 at.% Cr.

Table 1 recapitulates the quantitative results obtained from the structural analyses carried out in the course of investigations. Nanopowders with large specific surface area (SSA), as derived from BET, and the small crystallite size, as determined from XRD, have been obtained by FSS.

TEM images of the pure TiO_2, TiO_2:0.1 at.% Cr and TiO_2:1 at.% Cr nanopowders prepared using FSS technique are shown in Fig. 2. All the considered samples present the particle morphology typical for this method of synthesis. The particle size is of the order of 19-30 nm and decreases systematically with the increasing Cr composition. This is a consequence of a dilution effect, described in detail in [17].

Fig. 3 shows X-ray diffraction patterns of pure TiO_2 and TiO_2:Cr nanopowders at different Cr loadings (0.1 – 5 at.% Cr). As it can be seen, two polymorphic forms of TiO_2, namely rutile R and anatase A, are present. The fraction of anatase largely dominates over rutile, but the rutile amount increases slightly with the addition of Cr (see Table 1). There is no significant change in the crystallographic structure of TiO_2:Cr as compared with that of pure TiO_2 for Cr doping level not exceeding 1 at.%. Up to 5 at.% none of the secondary phases, neither chromium oxide nor chromium titanates, have been identified. This is compatible with the reported solubility limit of Cr^{3+} in TiO_2 [18] and the fact that ionic radii of Cr^{3+} and Ti^{4+} are very similar [19].

Figs. 4 and 5 demonstrate the changes in the electrical resistance *R* of TiO_2-based nanosensors upon interaction with the reducing gas H_2.

Fig. 4 presents the sensor characteristics as a function of time for the hydrogen concentration varied in steps from 50 ppm to 3000 ppm at the constant temperature of 350°C for pure TiO_2 and TiO_2 loaded with 0.1 at.% Cr and 5 at.% Cr. Large and reproducible responses of the sensors follow the step changes in H_2 concentration. Fig. 5 gives a comparison between the responses of pure TiO_2 and TiO_2 loaded with 0.1,

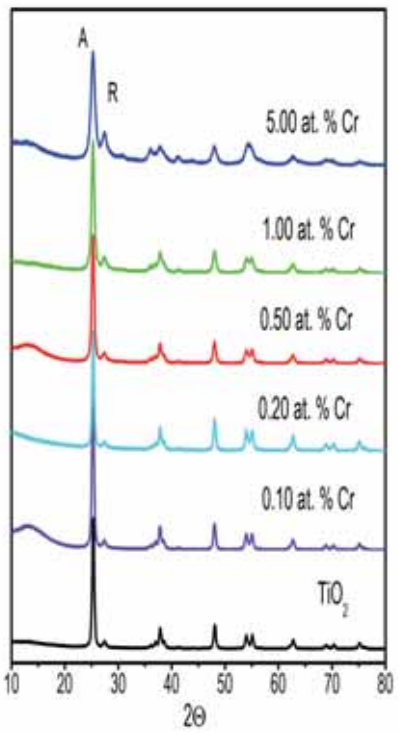

Fig. 3. X-ray diffraction patterns of TiO_2:Cr nanopowders at different Cr loadings.

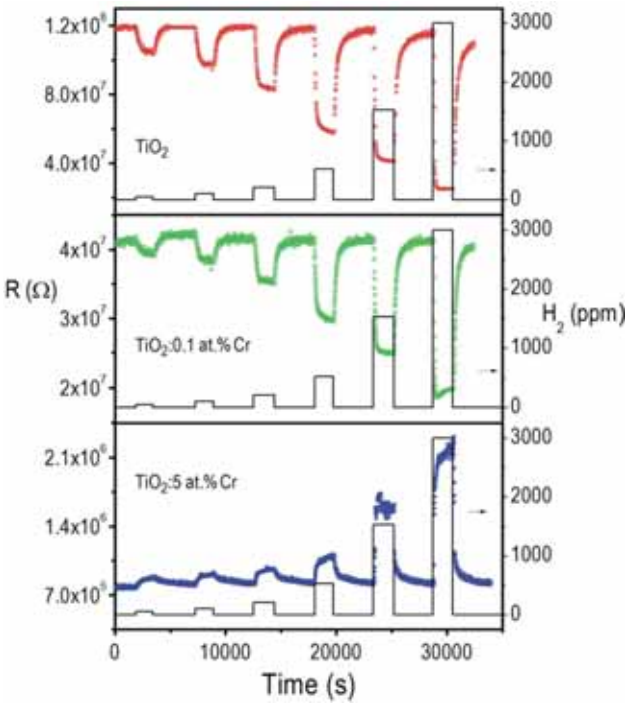

Fig. 4. Dynamic changes in the electrical resistance R of TiO_2:Cr sensors upon exposure to H_2 at 300°C. The programmed hydrogen concentration profile is given in steps (continuous black line).

0.2, 1 and 5 at.% Cr nanosensors at the same temperature of 350ºC to a single step change in hydrogen admission from 0 to 1500 ppm.

As we can see from the experimental data in Figs. 4 and 5, there is a systematic decrease in R for pure TiO_2 and TiO_2:Cr with up to 1 at.% Cr upon exposure to H_2, whereas for the TiO_2 nanosensor doped with 5 at.% Cr the electrical resistance R increases upon an interaction with H_2. Moreover, as shown in Fig. 4, the incorporation of Cr into TiO_2 causes a significant decrease in the initial electrical resistance R_0 of the material in air, *e.g.*, for the pure TiO_2 $R_0 = 1.2 \cdot 10^8\ \Omega$, for TiO_2: 0.1 at.% Cr $R_0 = 4 \cdot 10^7\ \Omega$ and for TiO_2: 5 at.% Cr $R_0 = 7 \cdot 10^5\ \Omega$ at 300ºC. Chromium dopant modifies the electronic structure of TiO_2 and forms localized acceptor levels in the forbidden band gap. This leads to the increase in the electron concentration and the decrease in the electrical resistance R_0 over a low-to-medium temperature range. The substitutional incorporation of Cr^{3+} can be described by the following reaction:

$$Cr_2O_3 \rightarrow 2Cr_{Ti} + V_O^{\bullet\bullet} + 3O_O + 2e', \qquad (2)$$

where Cr_{Ti} stands for the non-ionized chromium that substitutes for Ti in the lattice, $V_O^{\bullet\bullet}$ represents double ionized oxygen vacancy and e' is a quasi-free electron.

The sensor response S defined by Eq. (1) is given in Fig. 6 as a function of hydrogen concentration. The highest absolute value of the sensor response is obtained for both pure TiO_2 and TiO_2:Cr with 5 at.% Cr. To make a comparison, the absolute value of S should be considered since the change in the electrical resistance for TiO_2:Cr with 5 at.% Cr is positive, whereas all other investigated samples behave in the opposite way. The incorporation of chromium leads to the decrease in the sensor response in the case of TiO_2

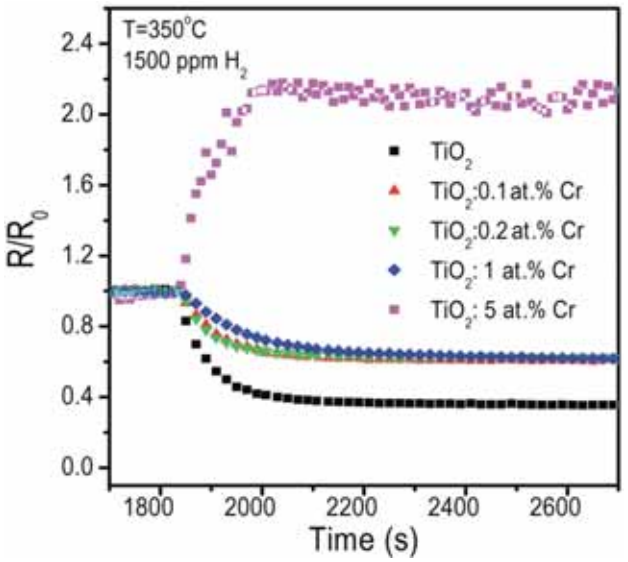

Fig. 5. The response of TiO_2:Cr sensors to a step change in the hydrogen concentration from 0 to 1500 ppm at 350°C.

nanosensors with 0.1, 0.2 and 1 at.% Cr, whereas for TiO_2 doped with 5 at.% Cr the response is highly improved.

Fig. 7 demonstrates the response S of the TiO_2:Cr nanosensors as a function the operating temperature for a given change in the hydrogen concentration (from 0 to 1500 ppm). As it can be noticed, with the decreasing temperature the sensor responses have a tendency to increase, what is especially important from the point of view of power consumption. For pure TiO_2 the lowest temperature at which the baseline resistance could be measured was 300ºC. This relatively high operating temperature for the pure TiO_2 can be lowered to 210-250ºC by adding Cr. Moreover, Cr incorporation enables to extend the temperature range under which the sensors work. The optimum operating temperature depends on the sensor composition. Taking into account the relatively low operating temperature the best, in terms of possible costs,

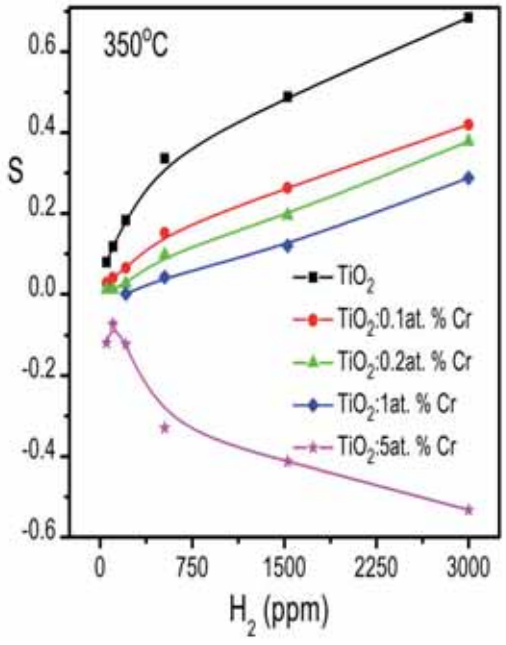

Fig. 6. The response S vs. H_2 concentration for TiO_2:Cr sensors at 350°C.

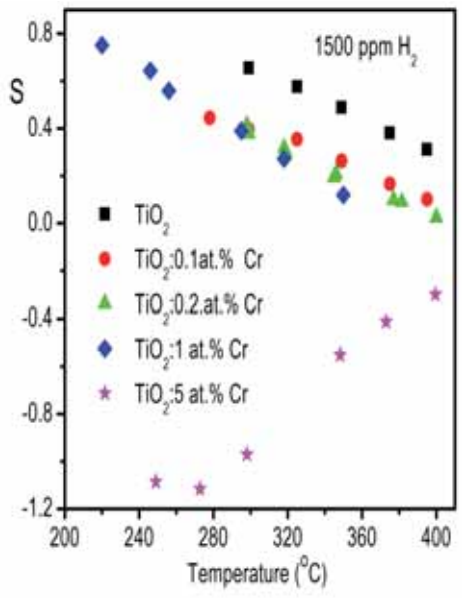

Fig. 7. The response S vs. operating temperature for TiO_2:Cr sensors.

candidates for commercial applications are TiO_2:1 at.% Cr and TiO_2:5 at.% Cr nanosensors.

4. Conclusions

The results obtained in the course of these studies allow the authors to formulate the following conclusions:

Crystalline nanopowders of mostly anatase TiO_2, grown by flame spray synthesis, are characterized by the large specific surface area and small crystallite size of the order of 9-27 nm depending on Cr loading.

Nanosensors obtained from TiO_2:Cr nanopowders show promising dynamic characteristics in response to hydrogen. The sensor responses S are large and reproducible.

The electrical resistance R decreases upon hydrogen exposure up to 1 at.% Cr while the reversed effect is observed at 5 at.% .

The sensor performance improves clearly with the decrease in the operating temperature. Incorporation of 1 at.% and 5 at.% of Cr into TiO_2 allows the measurable baseline resistance over the temperature range of 210-250°C to be reached, thus proving high sensor sensitivity to hydrogen.

Acknowledgements

This work was supported by the Polish Ministry of Education and Science (2009–2012) grant no. N N507 4665378.

References

[1] Göpel W., Jones T.A., Kleitz M., Lundsröm J., Seiyama T.: „Chemical and Biochemical Sensors" in Göpel, W., Schierbaum, K.D.: „Sensors", vol. 2, (Hrsg.) Verlag VCH, 1991.
[2] Chi Lu., Zhi Chen: „High-temperature resistive hydrogen sensor based on thin nanoporous rutile TiO_2 film on anodic aluminum oxide", Sens. Act. B, 140, (2009), 109-115.
[3] Zakrzewska K.: „Titanium Dioxide Thin Films for Gas Sensors and Photonic Applications", Uczelniane Wydawnictwa Naukowo-Dydaktyczne AGH, № 115, 2003, 1-223.
[4] Bernasik A., Radecka M., Rekas M., Sloma M.: „Electrical properties of Cr- and Nb- thin films", Appl. Surf. Sci., 65/66, (1993), 240-245.
[5] Sharma R.K., Bhatnagar M.C.: „Improvement of the oxygen gas sensitivity in doped TiO_2 thick films", Sens. Act. B, 56, (1999), 215-219.
[6] Zakrzewska K., Radecka M., Rekas M.: „Effect of Nb, Cr, Sn additions on gas sensing properies of TiO_2 thin films", Thin Solid Films, 310, (1997), 161-166.
[7] Sharma R.K., Bhatnagar M.C., Sharma G.L.: „Mechanism of highly sensitive and fast response Cr doped TiO_2 oxygen gas sensor", Sens. Act. B, 45, (1997), 209-215.
[8] Ruiz A.M., Sakai G., Cornet A., Shimanoe K., Morante J.R., Yamazoe N.: „Cr-doped TiO_2 gas sensor for exhaust NO_2 monitoring", Sens. Act. B, 93, (2003), 509-518.
[9] Li Y., Wlodarski W., Galatsis K., Moslih S.H., Cole J., Russo S., Rockelmann N.: „Gas sensing properties of *p*-type semiconducting Cr-doped TiO_2 thin films", Sens. Act. B, 83, (2002), 160-163.
[10] Alessandri I., Comini E., Bontempi E., Faglia G., Depero L. E., Sberveglieri G.: „Cr-inserted TiO_2 thin films for chemical gas sensors", Sens. Act. B, 128, (2007), 312-319.
[11] Lebrun A., Carpentier J-L, Perdu F., Tellier P.: „Comparative study of electronic conduction between pure and weakly chromium-doped rutile at 1273 K", Comptes Rendus de L'Academie des Sciences Serie II Mecanique Physique Chimie Sciences de L'Univers Sciences de la Terre, 28 (1987), 629-632.
[12] Carpentier J.-L., Lebrun A., Perdu F.: „Point defects and charge transport in pure and chromium-doped rutile at 1273 K", J. Phys. Chem. Solids., 50, (1989), 145-151.
[13] Radecka M., Rękas M.: „Defect structure and electrical properties of Cr- and Nb-doped TiO_2 thin films", Solid State Phen., 39-40, (1999), 135-138.
[14] Hooker S. A.: „Nanotechnology advantages applied to gas sensors development", The Nanoparticles 2002 Conference Proc., Business Communications Co., Inc., Norwalk, CT USA, 1-7.
[15] Comini E.: „Metal oxide nano-crystals for gas sensing", Anal. Chimica Acta, 568, (2006), 28-40.
[16] Trenczek-Zajac A., Radecka M., Jasinski M., Michalow K.A., Rekas M., Kusior E., Zakrzewska K., Heel A., Graule T., Kowalski K.: „Influence of Cr on the structural and optical properties of TiO_2:Cr nanopowders prepared by Flame Spray Synthesis (FSS)", J. Power Sour., 194, (2009), 104-111.
[17] Akurati K.K., Vital A., Fortunato G., Hany R., Nueesch F., Graule T.: „Flame synthesis of TiO_2 nanoparticles with high photocatalytic activity", Solid State Sci., 9, (2007), 247-257.
[18] Florke O.W., Lee C.W.: „Phase diagram TiO_2-Cr_2O_3", J. Solid State Chem., 1, (1969), 445-446.
[19] Shannon R.D.: „Revised effective ionic radii and systematic studies of interatomic distances in halides and chalcogenides", Acta Crystall., A32, (1976), 751-767.

♦

Received 1 March 2010; accepted 8 May 2010